Reversible Chelate-to-Bridge Ligand Exchange in $Co_2(CO)_4(\mu\text{-}PhC{\equiv}CPh)(bma)$ and Alkyne–Diphosphine Ligand Coupling. Synthesis, Reactivity, and Molecular Structures of $Co_2(CO)_4(\mu\text{-}PhC{\equiv}CPh)(bma)$, $Co_2(CO)_4(\mu\text{-}PhC{\equiv}CPh)\{(Z)\text{-}Ph_2PCH{=}CHPPh_2\}$, and $Co_2(CO)_4\{\eta^2,\eta^2,\eta^1,\eta^1\text{-}(Z)\text{-}Ph_2PC(Ph){=}(Ph)C\overline{C{=}C(PPh_2)C(O)OC}(O)\}$

Kaiyuan Yang, Simon G. Bott,* and Michael G. Richmond*

Center for Organometallic Research and Education, Department of Chemistry, University of North Texas, Denton, Texas 76203

Received March 16, 1994[⊗]

The reaction of the alkyne-bridged binuclear complex $Co_2(CO)_6(\mu\text{-}PhC{\equiv}CPh)$ (**1**) with the unsaturated diphosphine ligands 2,3-bis(diphenylphosphino)maleic anhydride (bma) and (Z)-$Ph_2PCH{=}CHPPh_2$ has been investigated. It is shown that the bma ligand reacts with **1** to give $Co_2(CO)_4(\mu\text{-}PhC{\equiv}CPh)(bma)$ (**2**) with a chelating bma ligand. Chelate-to-bridge bma ligand equilibration is promoted by photolysis and thermolysis conditions. This transformation proceeds by dissociative CO loss and with a K_{eq}(bridge/chelate) of ~1 at 45 °C. The binuclear complex $Co_2(CO)_4(\mu\text{-}PhC{\equiv}CPh)\{(Z)\text{-}Ph_2PCH{=}CHPPh_2\}$ (**3**) exhibits a chelating diphosphine ligand with no evidence for the analogous chelate-to-bridge exchange that was observed with **2**. The alkyne complex **2** undergoes P–C(maleic anhydride) ligand cleavage coupled with alkyne–C(maleic anhydride) and alkyne–PPh_2 bond formation at 83 °C to give $Co_2(CO)_4\{\eta^2,\eta^2,\eta^1,\eta^1\text{-}(Z)\text{-}Ph_2PC(Ph){=}C(Ph)\overline{C{=}C(PPh_2)C(O)OC}(O)\}$ (**4**). All complexes have been isolated and characterized in solution by IR and NMR spectroscopy. VT ^{13}C NMR measurements indicate that the ancillary CO groups in **2**–**4** are static with respect to intramolecular metal exchange over the temperature range −91 °C to room temperature. The solid-state structures of **2** (bridging), **3** (chelating), and **4** have been established by X-ray crystallography. Binuclear **2**, as the CH_2Cl_2 solvate, crystallizes in the triclinic space group $P\bar{1}$: $a = 10.712(1)$ Å, $b = 11.1467(8)$ Å, $c = 19.944(1)$ Å, $\alpha = 78.311(6)°$, $\beta = 89.029(7)°$, $\gamma = 68.169(7)°$, $V = 2160.4(3)$ Å^3, $Z = 2$, $d_{calc} = 1.475$ g·cm^{-3}; $R = 0.0697$, $R_w = 0.0850$ for 1711 observed reflections. **3** crystallizes in the triclinic space group $P\bar{1}$: $a = 9.983(2)$ Å, $b = 12.047(2)$ Å, $c = 16.651(2)$ Å, $\alpha = 74.67(1)°$, $\beta = 77.99(1)°$, $\gamma = 84.52(1)°$, $V = 1889.2(6)$ Å^3, $Z = 2$, $d_{calc} = 1.414$ g·cm^{-3}; $R = 0.0587$, $R_w = 0.0658$ for 2425 observed reflections. Compound **4** crystallizes in the orthorhombic space group $P2_12_12_1$: $a = 10.352(1)$ Å, $b = 15.883(1)$ Å, $c = 23.437(2)$ Å, $V = 3853.5(6)$ Å^3, $Z = 4$, $d_{calc} = 1.507$ g·cm^{-3}; $R = 0.0529$, $R_w = 0.0608$ for 1141 observed reflections. The eight-electron ligand 2-[(Z)-1,2-diphenyl-2-(diphenylphosphino)ethenyl]-3-(diphenylphosphino)maleic anhydride in **4** is bound to the two $Co(CO)_2$ moieties, forming an eight-membered dimetallocyclic ring. The redox properties of **2**–**4** have been examined by cyclic voltammetry. In the case of the chelating and bridging isomers of **2**, three well-defined one-electron responses were found and assigned to the 0/+1, 0/−1, and −1/−2 redox couples. IR analysis reveals that the unpaired electron in the reduced species $\mathbf{2}^{-\bullet}$ (chelating) resides primarily on the bma ligand. The nature of the HOMO and LUMO levels in **2** and **3** has been determined by extended Hückel MO calculations, the results of which are discussed with respect to the redox chemistry.

Introduction

The reactivity of transition-metal complexes possessing an ancillary alkyne ligand continues to be investigated by a diverse group of researchers.[1] While many metal–alkyne complexes are known, probably the most thoroughly studied class of alkyne complexes is that derived from dicobalt hexacarbonyl, i.e., $Co_2(CO)_6(\mu\text{-}alkyne)$.[2] Such complexes have found wide use in various organic transformations. For example, it has been demonstrated that cobalt-complexed propargyl cations function as propargyl cation synthons in carbon–carbon bond forming reactions,[3,4] while the protection of alkynes and the marking of acetylenic steroids by the

---

[⊗] Abstract published in *Advance ACS Abstracts,* August 15, 1994.

(1) (a) Nuel, D.; Dahan, F.; Mathieu, R. *J. Am. Chem. Soc.* **1985**, *107*, 1658. (b) Wang, J.; Sabat, M.; Lyons, L. J.; Shriver, D. F. *Inorg. Chem.* **1991**, *30*, 382. (c) Adams, R. D.; Babin, J. E.; Tasi, M.; Wolfe, T. A. *Organometallics* **1987**, *6*, 2228. (d) Adams, R. D.; Horváth, I. T. *Prog. Inorg. Chem.* **1985**, *32*, 127. (e) Templeton, J. L. *Adv. Organomet. Chem.* **1989**, *29*, 1. (f) Adams, R. D.; Chen, G.; Chen, L.; Wu, W.; Yin, J. *Organometallics* **1993**, *12*, 3431. (g) Bantel, H.; Powell, A. K.; Vahrenkamp, H. *Chem. Ber.* **1990**, *123*, 1607. (h) Green, M.; Jetha, N. K.; Mercer, R. J.; Norman, N. C.; Orpen, A. G. *J. Chem. Soc., Dalton Trans.* **1988**, 1843.

(2) Dickson, R. S.; Fraser, P. J. *Adv. Organomet. Chem.* **1974**, *12*, 323.

0276-7333/94/2313-3788$04.50/0

$Co_2(CO)_6$ moiety are routinely employed in organic syntheses[5] and biochemical receptor recognition studies,[6] respectively. Another well-known use of cobalt–alkyne compounds involves the cobalt-mediated ene-yne reaction, otherwise known as the Pauson–Khand reaction. Here complex carbocyclic ring systems are prepared regio- and stereospecifically under relatively mild conditions.[7]

Phosphine ligand substitution in $Co_2(CO)_6(\mu\text{-alkyne})$ has also been extensively studied from both mechanistic and theoretical aspects.[8] In the case of bidentate phosphine ligands both bridged and chelated products of the form $Co_2(CO)_{6-2n}(\mu\text{-alkyne})(L\text{-}L)_n$ (where $n = 1, 2$) are observed, with the exact product being dependent on the nature of the phosphine and the mode of binuclear complex activation.[9] Thermal ligand substitution with the common phosphines dppm and dppe yields the phosphine-bridged alkyne binuclear complexes, whereas electron transfer catalysis has been successfully utilized to give chelated or bridged complexes with impressive stereochemical control.[10] By comparison, ligand substitution studies with unsaturated diphosphine ligands have received less attention.[11]

Recently, we have examined the reaction between the tricobalt cluster $PhCCo_3(CO)_9$ and the diphosphine ligand 2,3-bis(diphenylphosphino)maleic anhydride (bma), which initially afforded the expected cluster $PhCCo_3(CO)_7(bma)$. Thermolysis or photolysis of this cluster led to the new cluster $Co_3(CO)_6\{\mu_2\text{-}\eta^2,\eta^1\text{-}C(Ph)C{=}C(PPh_2)C(O)OC(O)\}(\mu_2\text{-}PPh_2)$ as a result of P–C(maleic anhydride) bond cleavage coupled with C(μ-benzylidyne)–C(maleic anhydride) bond reductive elimination (eq 1).[12] The impetus for our current work stems from the isolobal relationship between $PhCCo_3(CO)_9$ and $Co_2(CO)_6(\mu\text{-}PhC{\equiv}CPh)$[13] and our desire to explore the generality of bma P–C(maleic anhydride) bond cleavage in different cluster systems.

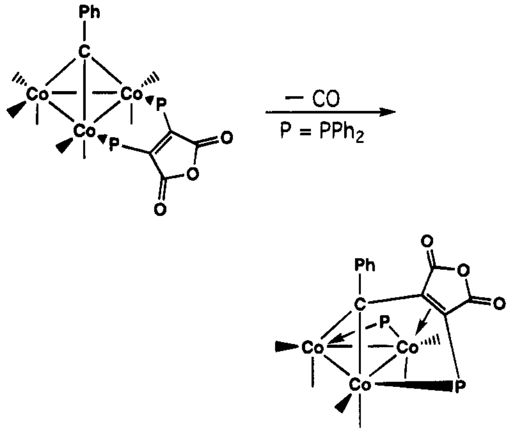

(1)

Here we report our results on the synthesis and characterization of $Co_2(CO)_4(\mu\text{-}PhC{\equiv}CPh)(bma)$ (**2**) and its transformation to $Co_2(CO)_4\{\eta^2,\eta^2,\eta^1,\eta^1\text{-}(Z)\text{-}Ph_2PC(Ph){=}C(Ph)C{=}C(PPh_2)C(O)OC(O)\}$ (**4**). The corresponding binuclear complex $Co_2(CO)_4(\mu\text{-}PhC{\equiv}CPh)\{(Z)\text{-}Ph_2PCH{=}CHPPh_2\}$ (**3**), prepared from **1** and the parent diphosphine ligand, has also been synthesized and studied under conditions analogous to **2** in order to highlight reactivity differences between **2** and **3**.

Results

I. Synthesis and Solution Characterization of $Co_2(CO)_4(\mu\text{-}PhC{\equiv}CPh)(bma)$ and $Co_2(CO)_4(\mu\text{-}PhC{\equiv}CPh)\{(Z)\text{-}Ph_2PCH{=}CHPPh_2\}$.

The reaction between $Co_2(CO)_6(\mu\text{-}PhC{\equiv}CPh)$ and bma was initially examined in CH_2Cl_2 at room temperature using the oxidative-decarbonylation reagent Me_3NO,[14] as a route to $Co_2(CO)_4(\mu\text{-}PhC{\equiv}CPh)(bma)$ (eq 2). A clean and immediate reaction was observed by IR analysis. TLC analysis revealed the presence of a small amount of starting material and product (>90%). The resulting green solution was purified by chromatography over silica gel to give pure **2** in yields of 50–60% as an air-sensitive solid. The low yields of isolated **2** compared to the solution reaction stem from the partial decomposition of **2** on the silica gel, presumably the result of anhydride ring hydrolysis.

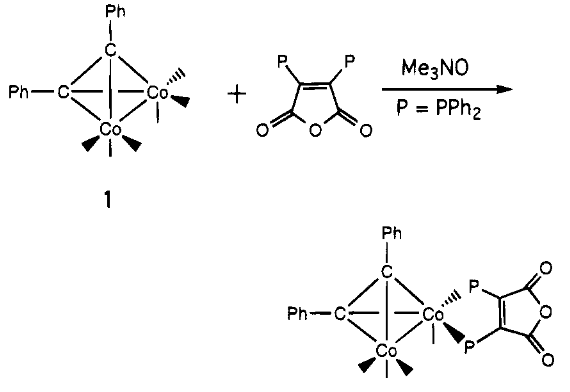

1

2 (chelating)

(2)

Two prominent terminal ν(CO) bands at 2047 (vs) and 1993 (vs) cm^{-1} were observed for **2** in CH_2Cl_2 solution,

---

(3) (a) Nicholas, K. M. *Acc. Chem. Res.* **1987**, *20*, 207. (b) Tester, R.; Varghese, V.; Montana, A. M.; Khan, M.; Nicholas, K. M. *J. Org. Chem.* **1990**, *55*, 186.

(4) Schreiber, S. L.; Klimas, M. T.; Sammakia, T. *J. Am. Chem. Soc.* **1987**, *109*, 5749.

(5) (a) Rubin, Y.; Knobler, C. B.; Diederich, F. *J. Am. Chem. Soc.* **1990**, *112*, 4966. (b) Melikyan, G. G.; Mineif, A.; Vostrowsky, O.; Bestmann, H. J. *Synthesis* **1991**, 633. (c) Osella, D.; Stein, E.; Jaouen, G.; Zanello, P. *J. Organomet. Chem.* **1991**, *401*, 37. (d) Osella, D.; Fiedler, J. *Organometallics* **1992**, *11*, 3875.

(6) Osella, D.; Dutto, G.; Jaouen, G.; Vessières, A.; Raithby, P. R.; De Benedetto, L.; McGlinchey, M. J. *Organometallics* **1993**, *12*, 4545.

(7) (a) Harrington, P. J. *Transition Metals in Total Synthesis*; John Wiley & Sons: New York, 1990, Chapter 9. (b) Krafft, M. E.; Juliano, C. A.; Scott, I. L.; Wright, C.; McEachin, M. D. *J. Am. Chem. Soc.* **1991**, *113*, 1693. (c) Krafft, M. E.; Scott, I. L.; Romero, R. H.; Feibelmann, S.; Van Pelt, C. E. *J. Am. Chem. Soc.* **1993**, *115*, 7199.

(8) (a) Heck, R. F. *J. Am. Chem. Soc.* **1963**, *85*, 657. (b) Aggarwal, R. P.; Connelly, N. G.; Crespo, M. C.; Dunne, B. J.; Hopkins, P. M.; Orpen, A. G. *J. Chem. Soc., Chem. Commun.* **1989**, 33. (c) Aggarwal, R. P.; Connelly, N. G.; Crespo, M. C.; Dunne, B. J.; Hopkins, P. M.; Orpen, A. G. *J. Chem. Soc., Dalton Trans.* **1992**, 655. (d) Arewgoda, C. M.; Robinson, B. H.; Simpson, J. *J. Chem. Soc., Chem. Commun.* **1982**, 284. (e) Arewgoda, M.; Robinson, B. H.; Simpson, J. *J. Am. Chem. Soc.* **1983**, *105*, 1893. (f) Casagrande, L. V.; Chen, T.; Rieger, P. H.; Robinson, B. H.; Simpson, J.; Visco, S. J. *Inorg. Chem.* **1984**, *23*, 2019.

(9) (a) Chia, L. S.; Cullen, W. R.; Franklin, M.; Manning, A. R. *Inorg. Chem.* **1975**, *14*, 2521. (b) Bird, P. H.; Fraser, A. R.; Hall, D. N. *Inorg. Chem.* **1977**, *16*, 1923. (c) Bianchini, C.; Dapporto, P.; Meli, A. *J. Organomet. Chem.* **1979**, *174*, 205.

(10) (a) Cunninghame, R. G.; Hanton, L. R.; Jensen, S. D.; Robinson, B. H.; Simpson, J. *Organometallics* **1987**, 1470. (b) Jensen, S. D.; Robinson, B. H.; Simpson, J. *Organometallics* **1987**, 1479.

(11) Crow, J. P.; Cullen, W. R. *Inorg. Chem.* **1971**, *10*, 2165.

(12) Yang, K.; Smith, J. M.; Bott, S. G.; Richmond, M. G. *Organometallics* **1993**, *12*, 4779.

(13) (a) Hoffmann, R. *Angew. Chem., Int. Ed. Engl.* **1982**, *21*, 711. (b) Albright, T. A.; Burdett, J. K.; Whangbo, M. H. *Orbital Interactions in Chemistry*; Wiley: New York, 1985.

(14) (a) Koelle, U. *J. Organomet. Chem.* **1977**, *133*, 53. (b) Albers, M. O.; Coville, N. *Coord. Chem. Rev.* **1984**, *53*, 227.

in addition to a weak shoulder at 1952 cm^{-1}. The symmetry of this IR spectrum is inconsistent with the IR data reported for other diphosphine-bridged $Co_2(CO)_6(\mu\text{-alkyne})$ complexes. Accordingly, the bma ligand was assigned to a chelating role in the chromatographed material. The expected $\nu(CO)$ bands associated with the bma ligand were observed at 1842 (w) and 1775 (s) cm^{-1} and ascribed to the vibrationally coupled asymmetric and symmetric bma carbonyl stretches, respectively.[15] These bands were insensitive to substitution by added ^{13}CO, consistent with their anhydride nature.

The $^{31}P\{^1H\}$ spectrum of **2** in $CDCl_3$ solution displayed a single resonance at ~ δ 60 over the temperature range of −56 °C to room temperature. The low-field location of the ^{31}P resonance supports the chelating nature of the bma ligand in **2**, as it is known that five-membered diphosphine−metal chelate rings experience a large nuclear deshielding of the ^{31}P centers, causing a lower field resonance relative to the alternative six-membered-ring isomer (vide infra).[16] The room temperature $^{13}C\{^1H\}$ NMR spectrum of ^{13}CO enriched **2** in THF exhibited two broad resonances at δ 207.5 and 201.1 in an integral ratio of 1:3, for the lone CO group at the bma-chelated cobalt center and the unsubstituted $Co(CO)_3$ center, respectively. Lowering the temperature to −91 °C led only to the sharpening of these resonances, as a result of the reduced molecular correlation time (τ_c), which is expected to afford sharper ^{13}C resonances.[17] The VT NMR data indicate that intramolecular carbonyl scrambling between the two cobalt centers is not important in **2**.

While the ^{31}P and ^{13}C NMR data clearly show that the sole product from the reaction between **1** and bma under Me_3NO-induced carbonyl activation is the chelating isomer of **2**, the thermolysis reaction between **1** and bma yields a mixture of chelating and bridging isomers of **2**. Refluxing an equimolar mixture of **1** and bma in CH_2Cl_2 overnight led to a more complicated IR spectrum, suggesting the existence of an isomeric mixture of bridging and chelating **2**. Examination of the $^{31}P\{^1H\}$ spectrum of the crude thermolysis product revealed the presence of two ^{31}P resonances at δ 60.6 and 30.3, assignable to the chelating and bridging isomers of **2**, respectively. The solubility of the bridging isomer of **2** in petroleum ether/CH_2Cl_2 (1:1) is slightly higher than that of the chelating isomer of **2**, and this allowed, after repeated recrystallizations, the isolation of small quantities of pure **2** (bridging) from the mother liquor. Three terminal $\nu(CO)$ bands at 2031 (s), 2009 (vs), and 1982 (sh) cm^{-1} are observed in the IR spectrum of this isomer, which are identical to the IR data reported for analogous dppm- and dppe-substituted complexes.[9,10] The $\nu(CO)$ bands at 1818 (w) and 1765 (s) cm^{-1} belong to the bridging bma ligand. The bridged isomer of **2** exhibits a $^{13}C\{^1H\}$ NMR spectrum with a broad carbonyl resonance at ~ δ 203 at room temperature, which upon cooling to −91 °C sharpens only slightly. Two separate carbonyl resonances were expected at low temperature given the NMR studies on related dppm-bridged cobalt−alkyne complexes published by Hansen.[18] In that report, dynamic ^{13}C NMR behavior is derived from a rocking motion of the coordinated acetylene ligand within the nido polyhedral core formed by the two cobalt centers. Two possible explanations for the low-temperature ^{13}C NMR behavior in **2** are reasonable, namely (1) a small chemical shift difference exists between the unique carbonyl groups or (2) the diphenylacetylene ligand is still rocking rapidly within the nido polyhedral core of **2**.

Since it was not immediately clear whether the formation of both of the isomers of **2** proceeded by separate pathways or if a chelate-to-bridge isomerization sequence was operative, we examined the thermolysis reaction of pure **2** (chelating). Refluxing **2** (chelating) in CH_2Cl_2 slowly afforded an isomeric mixture. The IR and ^{31}P NMR spectra were identical to those obtained from the reaction between **1** and bma (vide supra). The equilibrium nature of this reaction was also demonstrated by exploring the ratio of the bridging-to-chelating isomers of **2** by ^{31}P NMR spectroscopy. Heating a 0.03 M sample of **2** (chelating) in $CDCl_3$ in a sealed NMR tube at 45 °C for 48 h gave a K_{eq}(bridge/chelate) of ~1. No other phosphorus-containing products were observed in this reaction. The same results were also obtained when the equilibrium was approached by heating a 0.01 M sample of **2** (bridging) in dichloroethane overnight at 45 °C. Moreover, added CO strongly suppresses isomer equilibration. No isomerization was observed after 2 days at 45 °C when **2** (chelating) was stirred under 100 psi of CO. Consistent with the isomerization inhibition by CO is the fact that near-UV photolysis of **2** (chelating) also gives an isomeric mixture of **2**. Here optical excitation in the binuclear complex is expected to promote CO dissociation and, thus, initiates the isomerization sequence. Taken collectively, the ligand substitution data strongly support consecutive reaction pathways, where the initially formed chelating isomer gives rise to the corresponding bridging isomer as outlined in eq 3.

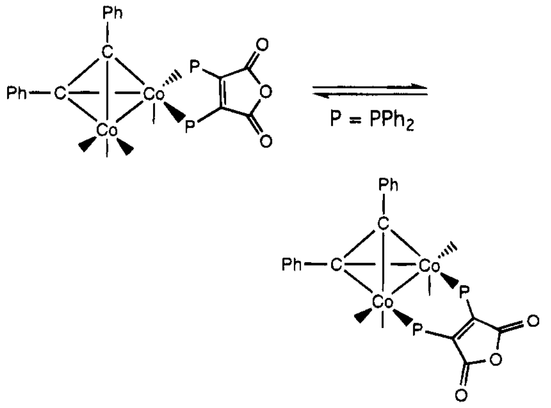

(3)

The reaction between **1** and (*Z*)-$Ph_2PCH{=}CHPPh_2$ was studied next because the anticipated product $Co_2(CO)_4(\mu\text{-}PhC{\equiv}CPh)\{(Z)\text{-}Ph_2PCH{=}CHPPh_2\}$, **3**, would allow us to probe for disparate reactivity between **2** and **3**. Since the binuclear complexes **2** and **3** are expected to be structurally similar, it could be argued that any observed reactivity differences would have their origin in the electronic properties inherent to each ancillary

---

[15] Dolphin, D.; Wick, A. *Tabulation of Infrared Spectral Data*; Wiley-Interscience: New York, 1977.

[16] (a) Garrou, P. E. *Chem. Rev.* **1981**, *81*, 229 and references therein. (b) Churchill, M. R.; Lashewycz, R. A.; Shapley, J. R.; Richter, S. I. *Inorg. Chem.* **1980**, *19*, 1277.

[17] (a) Mann, B. E.; Taylor, B. F. *^{13}C NMR Data for Organometallic Compounds*; Academic Press: New York, 1981. (b) Gragg, B. R.; Layton, W. J.; Niedenzu, K. *J. Organomet. Chem.* **1977**, *132*, 29. (c) Watson, W. H.; Nagl, A.; Hwang, S.; Richmond, M. G. *J. Organomet. Chem.* **1993**, *445*, 163.

[18] Hansen, B. E.; Mancini, J. S. *Inorg. Chem.* **1983**, *2*, 126.

diphosphine ligand. Complex **3** was obtained exclusively as the chelating isomer when **1** was allowed to react with (*Z*)-$Ph_2PCH{=}CHPPh_2$ in either dichloroethane at 50 °C or with Me_3NO in CH_2Cl_2 at room temperature (eq 4). The IR spectrum of **3** exhibits two terminal ν(CO) bands at 2039 (vs) and 1983 (vs) cm^{-1}. These ν(CO) bands are ~10 cm^{-1} lower in energy than the analogous carbonyl bands in **2** (chelating), which reflects the better donor properties of the (*Z*)-$Ph_2PCH{=}CHPPh_2$ ligand relative to the bma ligand, with its electron-withdrawing anhydride ring.[19] The chelating nature of the ancillary diphosphine was ascertained by ^{31}P and ^{13}C NMR spectroscopies, where a single resonance at δ 71.8 and two resonances at δ 208.8 (1C) and 202.8 (3C), respectively, have been recorded at −91 °C in THF solution.

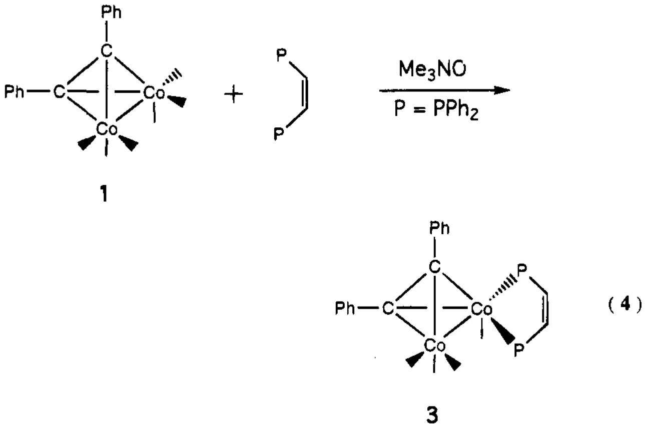

The thermolysis and photolysis reactivity of **3** under conditions comparable to those employed in the isomerization of **2** did not afford any of the bridging isomer of **3**. In both cases the only observed reaction was the decomposition of **3**, with decomposition from the thermolysis reaction being more extensive than that from the photolysis reaction. The absence of isomerization in **3** suggests that the diphosphine remains associated with the cobalt center and does not become free, a condition that would be required for isomerization.

II. Synthesis and Solution Characterization of $Co_2(CO)_4\{\eta^2,\eta^2,\eta^1,\eta^1$-(Z)-$Ph_2PC(Ph){=}(Ph)CC{=}C(PPh_2)C(O)OC(O)\}$.

During the course of investigating the isomerization of **2** in refluxing dichloroethane or toluene solutions we found the appearance of a new product by IR and TLC analyses. It was subsequently found that at temperatures higher than 75 °C **2** was unstable, giving as the only isolable product the new binuclear complex $Co_2(CO)_4\{\eta^2,\eta^2,\eta^1,\eta^1$-(*Z*)-$Ph_2PC(Ph){=}(Ph)C$-$C{=}C(PPh_2)C(O)OC(O)\}$, **4**, as shown in eq 5. This same product is obtained from the reaction between $Co_2(CO)_6(\mu$-PhC≡CPh) and bma in refluxing dichloroethane, by way of $Co_2(CO)_4(\mu$-PhC≡CPh)(bma). **4**, which results from the formal coupling of the diphenylacetylene and bma ligands, was isolated in 10% yield by column chromatography and characterized in solution by IR and NMR spectroscopies. When the thermolysis reaction was repeated under CO (100 psi) using either isomer of **2**, no reaction was observed. Only unreacted starting material was isolated at the end of these reactions.

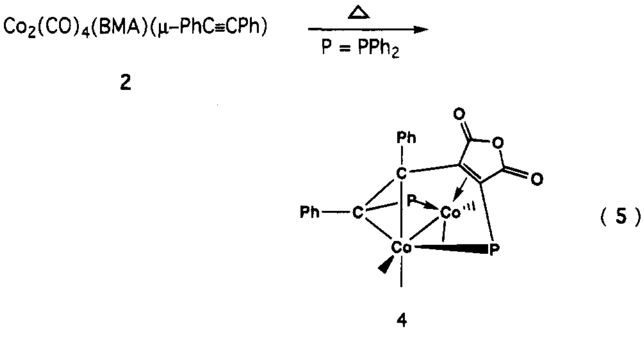

The IR spectrum in CH_2Cl_2 shows four terminal ν(CO) bands at 2050 (s), 2025 (vs), 2008 (s), and 1981 (m) cm^{-1}, in agreement with the highly asymmetric structure of this binuclear complex which should yield a greater number of carbonyl stretching bands relative to the starting bma-substituted complex **2**. The ν(CO) bands derived from the bma ligand are observed at 1809 (w) and 1745 (m) cm^{-1}. While the location of these latter two bands should be able to serve as indicators for P—C(maleic anhydride) bond cleavage reactivity, there are not enough examples of such transformations with this ligand that would allow us to make reactivity generalizations at the present time.

At −91 °C four equal-intensity carbonyl resonances were observed at δ 202.1, 201.1 (d, *J* = 15.3 Hz), 196.9, and 193.7 in the $^{13}C\{^1H\}$ NMR spectrum of **4**. The doublet resonance at δ 201.1 is presumed to result from coupling with one of the phosphine atoms in **4**. The ^{31}P NMR spectrum of **4** recorded under comparable conditions shows the presence of two inequivalent phosphine ligands at δ 46.7 (broad) and 27.8 (d, *J* = 17.0 Hz). While no attempt has been made to assign the ^{13}C and ^{31}P resonances to specific groups, we note that the NMR data are consistent with the structure of **4**. Warming these samples to room temperature led only to the broadening of these resonances as ^{59}Co quadrupolar-induced line broadening becomes more pronounced.

III. X-ray Diffraction Structures for $Co_2(CO)_4(\mu$-PhC≡CPh)(bma), $Co_2(CO)_4(\mu$-PhC≡CPh){(Z)-$Ph_2PCH{=}CHPPh_2$}, and $Co_2(CO)_4\{\eta^2,\eta^2,\eta^1,\eta^1$-(Z)-$Ph_2PC(Ph){=}(Ph)CC{=}C(PPh_2)C(O)OC(O)\}$.

The molecular structures of **2** (bridging), **3**, and **4** were established by X-ray diffraction analysis. All three binuclear complexes exist as discrete molecules in the unit cell with no unusually short inter- or intramolecular contacts. Table 1 lists the X-ray data collection and processing parameters, while Tables 2 and 3 give the atomic coordinates and selected distances and angles, respectively, for the complexes under study. The ORTEP diagrams are shown in Figure 1.

The binuclear complexes **2** (bridging) and **3** are structurally similar with respect to the polyhedral (μ-alkyne)Co_2 core, the only significant difference being the bonding mode adopted by the ancillary diphosphine ligand. Several attempts were made to grow single crystals of the chelating isomer of **2**; however, these attempts were not successful, yielding only twinned and amorphous crystals, which necessitated the structural characterization of the bridging isomer of **2**. Both **2** and **3** have a (μ-PhC≡CPh)Co_2 tetrahedral core, where the Co—Co bond length of 2.469(4) Å in **2** and 2.594(4) Å in **3** is comparable to other crystallographically characterized Co_2 binuclear complexes.[20] The 0.125 Å longer Co—Co bond in **3** (relative to **2**) results from the

---

[19] Lukehart, C. M. *Fundamental Transition Metal Organometallic Chemistry*; Brooks/Cole Publishing: Monterey, CA, 1985.

Table 1. X-ray Crystallographic Data and Processing Parameters

	2 (bridging)	**3**	**4**
space group	$P\bar{1}$, triclinic	$P\bar{1}$, triclinic	$P2_12_12_1$, orthorhombic
a, Å	10.712(1)	9.993(2)	10.352(1)
b, Å	11.1467(8)	12.047(2)	15.883(1)
c, Å	19.944(1)	16.651(2)	23.437(2)
α, deg	78.311(6)	74.67(1)	
β, deg	89.029(7)	77.99(1)	
γ, deg	68.169(7)	84.52(1)	
V, Å^3	2160.4(3)	1889.2(6)	3853.5(6)
mol formula	$C_{47}H_{32}Cl_2$-$Co_2O_7P_2$	$C_{44}H_{32}Co_2$-O_4P_2	$C_{46}H_{30}Co_2$-O_7P_2
fw	959.49	804.56	874.56
formula units per cell (Z)	2	2	4
ϱ, g·cm^{-3}	1.475	1.414	1.507
abs coeff (μ), cm^{-1}	10.13	10.00	9.92
λ (Mo Kα), Å	0.710 73	0.710 73	0.710 73
collecn range, deg	$2.0 \le 2\theta \le 44.0$	$2.0 \le 2\theta \le 44.0$	$2.0 \le 2\theta \le 44.0$
max scan time, s	120	120	120
scan speed range, deg·min^{-1}	0.67−8.0	0.67−8.0	0.67−8.0
tot. no. of data collcd	5230	4636	2694
no. of indep data, $I > 3\sigma(I)$	1711	2425	1141
R	0.0697	0.0587	0.0529
R_w	0.085	0.0658	0.0608
weights	$[0.04F^2 + (\sigma F)^2]^{-1}$	$[0.04F^2 + (\sigma F)^2]^{-1}$	$[0.04F^2 + (\sigma F)^2]^{-1}$

chelating diphosphine ligand, which exerts a steric destabilization on the cobalt core, manifesting itself in an elongation of the Co—Co bond.[21] The ancillary CO and diphosphine ligands occupy sites in each complex that give rise to the commonly observed "sawhorse" geometry associated with the Co_2L_6 fragment in **2** and **3**.[22] Considering each cobalt atom as defining a distorted octahedron, with a ligand sphere consisting of a shared diphenylacetylene ligand, CO/P ligands, and a Co—Co bond, allows for a ready description of the ancillary CO/P ligands at a given cobalt center. In **2**, each cobalt atom possesses a pseudoequatorial phosphine and CO ligand and a single pseudoaxial CO group. Similar ligand arrangements have been observed in other diphosphine-bridged binuclear complexes of this genre.[9,10] Neglecting the alkyne ligand, a view down the Co—Co bond generates a nearly eclipsed Newman projection (i.e., "sawhorse" conformation) defined by the CO/P ligands at each cobalt center. The unique pseudoaxial ligand in such a projection is defined by the ligand that bisects the alkyne moiety. Complex **3** is similar to **2**, except that the chelating diphosphine ligand occupies a pseudoaxial (P(1)) and pseudoequatorial (P(2)) at the same cobalt center. The bond distances and angles in these two binuclear complexes exhibit no unusual properties that merit a detailed discussion.

The structure of **4** consists of a $Co_2(CO)_4$ core that is ligated by the eight-electron ligand 2-[(*Z*)-1,2-diphenyl-2-(diphenylphosphino)ethenyl]-3-(diphenylphosphino)-maleic anhydride. A picture of the isolated ligand is shown as follows:

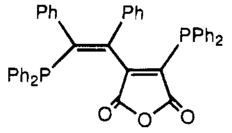

The Co—Co bond length of 2.594(4) Å in **4** is in agreement with other complexes with a Co—Co single bond.[20] The two Co—P bond lengths of 2.244(6) Å for the Co(1)—P(1) and 2.179(6) Å for the Co(2)—P(2) bonds are normal in comparison to other phosphine-substituted cobalt complexes,[23] but it is notable that the shorter Co—P distance corresponds to the PPh_2 group that is attached to the electron-withdrawing maleic anhydride ring. The alkene bonds of the ethene and maleic anhydride ligands are bound to different cobalt atoms in an η^2 fashion, with the adjacent PPh_2 group of each alkene being bound to the opposite cobalt atom in a typical η^1 fashion. The complexation of this eight-electron ligand to the two $Co(CO)_2$ moieties results in the formation of an eight-membered dimetallocyclic ring. The X-ray structure is important as it reveals that the two phenyl groups that were originally from the diphenylacetylene ligand are situated cis to each other, as are the PPh_2 and (diphenylphosphino)maleic anhydride groups.

IV. Cyclic Voltammetric Investigations of the Binuclear Complexes 2−4. The electrochemical behavior of **2**−**4** was next examined as part of our interest in redox-active polynuclear systems and systems that bear a pendant redox-active ligand.[17c] Here the binuclear complexes with the bma ligand would be expected to display redox properties different from the analogous phosphine-substituted $Co_2(CO)_{6-n}(\mu$-alkyne)-P_n systems (where $n = 1, 2$).[8b−g,10,24]

The cyclic voltammetry studies were conducted in CH_2Cl_2 containing 0.1 M tetra-*n*-butylammonium perchlorate (TBAP) as the supporting electrolyte at a platinum electrode. The two isomers of **2** allow for a direct comparison regarding the redox properties as a function of the coordination mode adopted by the bma ligand. Both of these isomers display three well-defined redox responses as shown in the cyclic voltammograms (CV) in Figure 2, while Table 4 gives the pertinent potential data for all of the systems studied. The 0/−1 redox couple in both isomers of **2** is reversible on the basis of the peak current (I_p^a/I_p^c) ratios of unity and plots of the current function (I_p) vs the square root of the scan rate (v), which were linear over the scan rates examined.[25] Calibration of the peak currents against ferrocene using Walden's rule also supports the one-electron nature of the couple.[25] The second reduction step is less reversible as judged by the diminished current ratio of 0.58 and 0.88 for the chelating and bridging isomers, respectively. The reduction waves of both isomers exhibit only slight potential differences, and no significance is attached to these potentials as a function of the coordination mode of the bma ligand.

---

[20] (a) Cotton, F. A.; Jamerson, J. D.; Stults, B. R. *J. Am. Chem. Soc.* **1976**, *98*, 1774. (b) Mirza, H. A.; Vittal, J. J.; Puddephatt, R. J.; Frampton, C. S.; Manojlović-Muir, L.; Xia, W.; Hill, R. H. *Organometallics* **1993**, *12*, 2767. (c) Gregson, D.; Howard, J. A. K. *Acta Crystallogr.* **1983**, *C39*, 1024. (d) Lang, H.; Zsolnai, L. *Chem. Ber.* **1991**, *124*, 259. (e) Gelling, A.; Jeffery, J. C.; Povey, D. C.; Went, M. J. *J. Chem. Soc., Chem. Commun.* **1991**, 349.

[21] Richmond, M. G.; Kochi, J. K. *Organometallics* **1987**, *6*, 254.

[22] Thorn, D. L.; Hoffmann, R. *Inorg. Chem.* **1978**, *17*, 126.

[23] (a) Don, M.-J.; Richmond, M. G.; Watson, W. H.; Krawiec, M.; Kashyap, R. P. *J. Organomet. Chem.* **1991**, *418*, 231. (b) Yang, K.; Bott, S. G.; Richmond, M. G. *J. Organomet. Chem.* **1993**, *454*, 273. (c) Brice, M. D.; Penfold, B. R.; Robinson, W. T.; Taylor, S. R. *Inorg. Chem.* **1970**, *9*, 362. (d) Balavoine, G.; Collin, J.; Bonnet, J. J.; Lavigne, G. *J. Organomet. Chem.* **1985**, *280*, 429.

[24] For bma-related redox chemistry, see: (a) Mao, F.; Tyler, D. R.; Keszler, D. *J. Am. Chem. Soc.* **1989**, *111*, 130. (b) Mao, F.; Philbin, C. E.; Weakley, T. J. R.; Tyler, D. R. *Organometallics* **1990**, *9*, 1510.

[25] (a) Bard, A. J.; Faulkner, L. R. *Electrochemical Methods*; Wiley: New York, 1980. (b) Adams, R. N. *Electrochemistry at Solid Electrodes*; Marcel Dekker: New York, 1969.

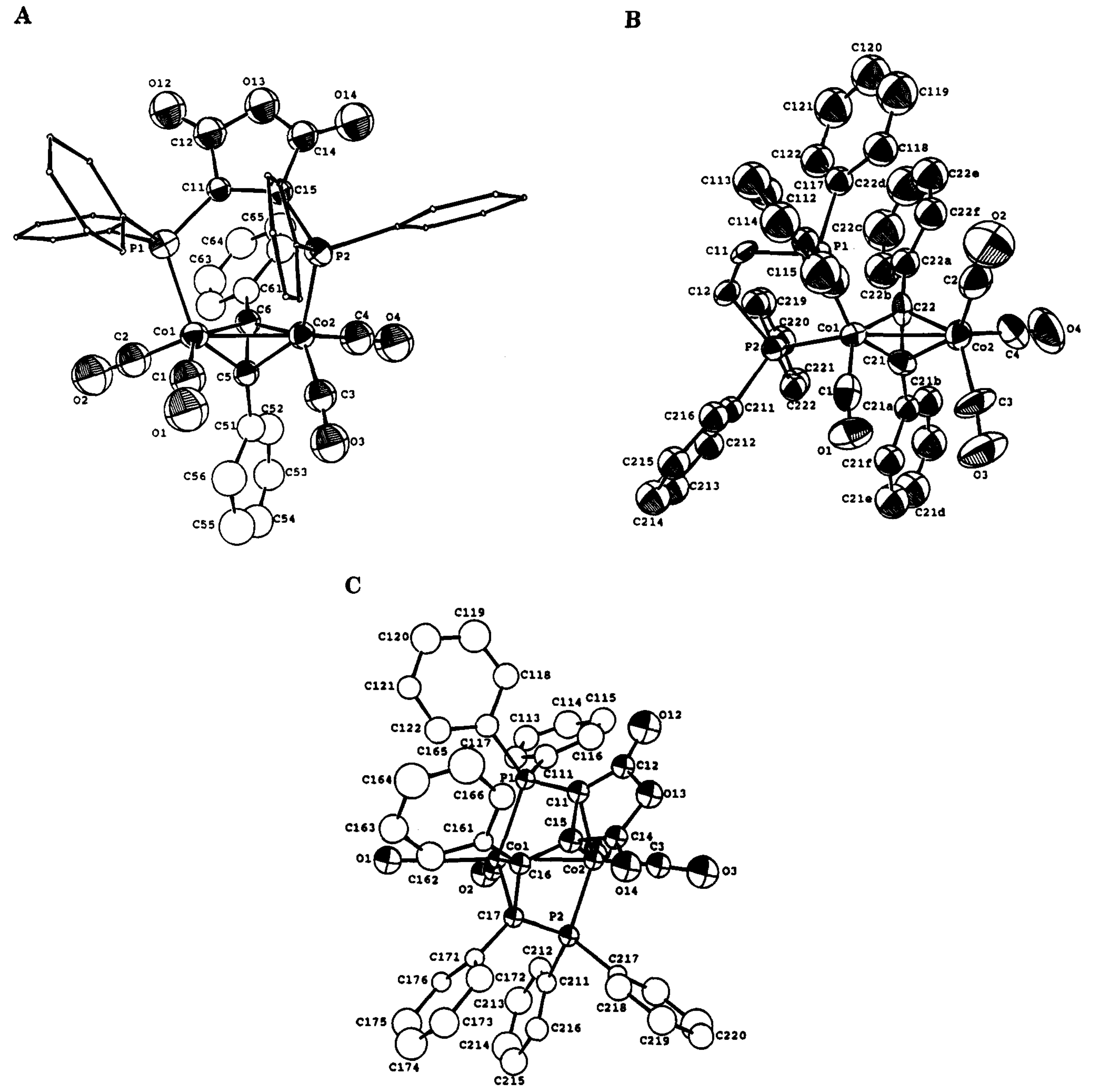

Figure 1. ORTEP drawings of the non-hydrogen atoms of (A) $Co_2(CO)_4(\mu\text{-}PhC{\equiv}CPh)(bma)$, (B) $Co_2(CO)_4(\mu\text{-}PhC{\equiv}CPh)\{(Z)\text{-}Ph_2PCH{=}CHPPh_2\}$, and (C) $Co_2(CO)_4\{\eta^2,\eta^2,\eta^1,\eta^1\text{-}(Z)\text{-}Ph_2PC(Ph){=}(Ph)CC{=}C(PPh_2)C(O)OC(O)\}$. Thermal ellipsoids are drawn at the 50% probability level.

How the bma ligand coordinates to the binuclear complex does, however, affect the potential of the 0/+1 redox couple. It can be seen that **2** (chelating) is oxidized at 0.13 V more positive than **2** (bridging). To our knowledge, such an effect has not been previously reported for a binuclear complex.[26] The 0/+1 wave in both isomers is only partially reversible, as the current ratio (I_p^c/I_p^a) for both isomers is ~0.8. Decomposition of the radical cation gives rise to the small amount of unknown material in the CV at −0.05 V (Figure 2A) and 0.01 V (Figure 2B). Lowering the temperature to 0 °C renders the oxidation wave fully reversible.

The CV of **3** (not shown) reveals the presence of an oxidation wave at $E_{1/2} = 0.22$ V that is not completely reversible in a chemical sense given a current ratio (I_p^c/I_p^a) of ~0.50. No reduction wave was observed when the CV was scanned within the reductive potential range of CH_2Cl_2. The lack of a reduction wave(s) in **3** is consistent with the data reported for other diphosphine-substituted complexes of this genre,[10] as the LUMO is predicted to be an antibonding Co−Co orbital.[27,28] Since each isomer of **2** displays an initial reduction wave ~−0.55 V, this suggests that the bma ligand is the site of electron accession, a fact supported

---

[26] For examples of redox-dependent structures involving cis- and trans-isomers and fac- and mer-isomers of mononuclear complexes, see: (a) Bond, A. M.; Colton, R.; McCormick, M. J. *Inorg. Chem.* **1977**, *16*, 155. (b) Sullivan, B. P.; Meyer, T. J. *Inorg. Chem.* **1982**, *21*, 1037. (c) Rieke, R. D.; Kojima, H.; Saji, T.; Rechberger, P.; Öfele, K. *Organometallics* **1988**, *7*, 749. (d) Vallat, A.; Person, M.; Rollier, L.; Laviron, E. *Inorg. Chem.* **1987**, *26*, 332. (e) Conner, K. A.; Walton, R. A. *Inorg. Chem.* **1986**, *25*, 4422. (f) Lilga, M. A.; Ibers, J. A. *Inorg. Chem.* **1984**, *23*, 3538. (g) Bagchi, R. N.; Bond, A. M.; Brain, G.; Colton, R.; Henderson, T. L. E.; Kevekordes, J. E. *Organometallics* **1984**, *3*, 4. (h) Carriedo, G. A.; Connelly, N. G.; Perez-Carreno, E.; Orpen, A. G.; Rieger, A. L.; Rieger, P. H.; Riera, V.; Rosair, G. M. *J. Chem. Soc., Dalton Trans.* **1993**, 3103.

Table 2. Positional Parameters for Non-Hydrogen Atoms of the Binuclear Complexes 2-4 with Estimated Standard Deviations in Parentheses[a]

atom	*x*	*y*	*z*	*B*, Å^2	atom	*x*	*y*	*z*	*B*, Å^2
$Co_2(CO)_4(\mu\text{-}PhC{\equiv}CPh)(bma){\cdot}CH_2Cl_2$ (Bridging Isomer)									
Co(1)	0.0401(3)	−0.0196(3)	0.2274(2)	3.21(7)	C(66)	−0.297(2)	−0.129(2)	0.205(1)	4.0(5)*
Co(2)	−0.1409(3)	0.0258(3)	0.3081(1)	2.97(7)	C(111)	0.152(2)	−0.275(2)	0.152(1)	4.2(5)*
P(1)	0.1392(6)	−0.2375(5)	0.2388(3)	3.3(1)	C(112)	0.265(2)	−0.282(2)	0.119(1)	4.5(5)*
P(2)	−0.0575(5)	−0.1682(5)	0.3806(3)	2.9(1)	C(113)	0.265(2)	−0.292(2)	0.046(1)	6.3(7)*
O(1)	0.202(2)	0.079(2)	0.3006(9)	7.0(5)*	C(114)	0.159(2)	−0.300(2)	0.016(1)	5.8(6)*
O(2)	0.119(2)	0.051(2)	0.0903(9)	7.5(5)*	C(115)	0.045(2)	−0.294(2)	0.053(2)	5.7(6)*
O(3)	−0.093(1)	0.227(1)	0.3627(8)	5.7(4)*	C(116)	0.044(2)	−0.280(2)	0.119(1)	4.4(5)*
O(4)	−0.426(2)	0.119(2)	0.3208(9)	6.8(4)*	C(117)	0.312(2)	−0.332(2)	0.276(1)	4.3(5)*
O(12)	0.103(1)	−0.526(1)	0.2344(8)	5.9(4)*	C(118)	0.383(2)	−0.459(2)	0.268(1)	6.2(7)*
O(13)	−0.041(1)	−0.497(1)	0.3159(8)	5.1(4)*	C(119)	0.517(3)	−0.530(3)	0.292(1)	7.2(7)*
O(14)	−0.155(2)	−0.427(1)	0.4033(8)	6.0(4)*	C(120)	0.574(2)	−0.467(2)	0.329(1)	5.1(6)*
C(1)	0.142(2)	0.038(2)	0.271(1)	4.9(6)*	C(121)	0.509(2)	−0.342(2)	0.342(1)	5.5(6)*
C(2)	0.087(2)	0.023(2)	0.147(1)	5.3(6)*	C(122)	0.376(2)	−0.274(2)	0.313(1)	4.4(5)*
C(3)	−0.107(2)	0.139(2)	0.347(1)	3.9(5)*	C(211)	−0.163(2)	−0.194(2)	0.450(1)	3.0(4)*
C(4)	−0.305(2)	0.075(2)	0.318(1)	5.1(6)*	C(212)	−0.117(2)	−0.234(2)	0.518(1)	4.4(5)*
C(5)	−0.139(2)	0.112(2)	0.215(1)	2.9(4)*	C(213)	−0.199(2)	−0.241(2)	0.568(1)	5.7(6)*
C(6)	−0.153(2)	0.003(2)	0.215(1)	2.9(4)*	C(214)	−0.339(3)	−0.207(2)	0.553(1)	6.8(7)*
C(11)	0.049(2)	−0.333(2)	0.2853(9)	2.4(4)*	C(215)	−0.379(2)	−0.172(2)	0.484(1)	6.3(7)*
C(12)	0.046(2)	−0.459(2)	0.273(1)	4.6(5)*	C(216)	−0.299(2)	−0.162(2)	0.433(1)	3.8(5)*
C(14)	−0.080(2)	−0.415(2)	0.358(1)	3.9(5)*	C(217)	0.106(2)	−0.218(2)	0.427(1)	3.4(5)*
C(15)	−0.032(2)	−0.305(2)	0.3411(9)	2.6(4)*	C(218)	0.145(2)	−0.124(2)	0.446(1)	3.8(5)*
C(51)	−0.210(2)	0.256(2)	0.181(1)	3.6(5)*	C(219)	0.264(2)	−0.158(2)	0.486(1)	3.9(5)*
C(52)	−0.336(2)	0.302(2)	0.146(1)	4.9(6)*	C(220)	0.336(2)	−0.288(2)	0.509(1)	4.6(5)*
C(53)	−0.397(2)	0.431(2)	0.112(1)	4.9(6)*	C(221)	0.305(2)	−0.387(2)	0.492(1)	4.9(6)*
C(54)	−0.342(2)	0.518(2)	0.114(1)	5.3(6)*	C(222)	0.188(2)	−0.354(2)	0.449(1)	4.5(5)*
C(55)	−0.217(2)	0.480(2)	0.144(1)	6.1(6)*	Cl(1)	0.352(2)	0.226(2)	0.187(1)	10.6(7)*
C(56)	−0.140(2)	0.343(2)	0.176(1)	5.4(6)*	Cl(2)	0.231(4)	0.353(4)	0.045(2)	13(1)*
C(61)	−0.229(2)	−0.049(2)	0.176(1)	3.4(5)*	Cl(3)	0.380(3)	0.141(3)	0.153(1)	13.0(8)*
C(62)	−0.241(2)	−0.012(2)	0.104(1)	4.5(5)*	Cl(4)	0.128(5)	0.357(4)	0.084(2)	17(2)*
C(63)	−0.316(2)	−0.052(2)	0.063(1)	5.8(6)*	Cl(5)	0.313(3)	0.319(3)	0.044(2)	9.3(8)*
C(64)	−0.376(2)	−0.131(2)	0.093(1)	5.5(6)*	Cl(6)	0.382(4)	0.226(4)	0.080(2)	15(1)*
C(65)	−0.377(2)	−0.163(2)	0.167(1)	5.2(6)*	C(1S)	0.258(4)	0.332(3)	0.126(2)	12(1)*
$Co_2(CO)_4(\mu\text{-}PhC{\equiv}CPh)\{(Z)\text{-}Ph_2PCH{=}CHPPh_2\}$									
Co(1)	0.6308(1)	0.3429(1)	0.70036(9)	2.64(3)	C(22e)	0.775(2)	0.284(1)	1.000(1)	7.2(4)*
Co(2)	0.4268(2)	0.3334(1)	0.8161(1)	3.69(4)	C(22f)	0.691(1)	0.310(1)	0.9392(8)	5.2(3)*
P(1)	0.7595(3)	0.4922(2)	0.6846(2)	2.84(6)	C(111)	0.719(1)	0.6365(8)	0.6230(6)	2.8(2)*
P(2)	0.8081(3)	0.2656(2)	0.6296(2)	2.81(6)	C(112)	0.816(1)	0.721(1)	0.5962(7)	4.0(3)*
O(1)	0.4576(8)	0.4032(7)	0.5724(5)	5.4(2)	C(113)	0.789(1)	0.829(1)	0.5477(8)	4.6(3)*
O(2)	0.410(1)	0.5709(8)	0.8312(8)	10.1(4)	C(114)	0.663(1)	0.854(1)	0.5234(8)	4.9(3)*
O(3)	0.2154(9)	0.3230(9)	0.7215(7)	8.3(3)	C(115)	0.568(1)	0.774(1)	0.5489(8)	5.3(3)*
O(4)	0.302(1)	0.200(1)	0.9812(6)	9.5(4)	C(116)	0.596(1)	0.665(1)	0.5990(7)	4.2(3)*
C(1)	0.534(1)	0.3823(9)	0.6182(7)	3.9(3)	C(117)	0.817(1)	0.5279(9)	0.7724(7)	3.4(2)*
C(2)	0.418(1)	0.477(1)	0.8253(9)	5.5(4)	C(118)	0.745(1)	0.607(1)	0.8122(8)	4.8(3)*
C(3)	0.293(1)	0.330(1)	0.7602(9)	5.7(3)	C(119)	0.792(2)	0.634(1)	0.878(1)	7.0(4)*
C(4)	0.351(1)	0.257(1)	0.9146(8)	6.3(4)	C(120)	0.906(2)	0.583(1)	0.9006(9)	6.8(4)*
C(11)	0.9231(9)	0.4613(8)	0.6232(6)	2.8(2)	C(121)	0.978(2)	0.502(1)	0.8652(9)	6.8(4)*
C(12)	0.947(1)	0.3636(9)	0.6007(7)	3.4(3)	C(122)	0.932(1)	0.472(1)	0.7996(8)	5.2(3)*
C(21)	0.548(1)	0.2078(9)	0.7790(7)	3.4(3)	C(211)	0.800(1)	0.2531(8)	0.5231(6)	2.7(2)*
C(21a)	0.507(1)	0.0968(9)	0.7792(7)	3.2(2)*	C(212)	0.837(1)	0.1518(9)	0.4964(7)	3.8(2)*
C(21b)	0.508(1)	0.005(1)	0.8484(8)	4.8(3)*	C(213)	0.836(1)	0.153(1)	0.4128(8)	4.7(3)*
C(21c)	0.474(2)	−0.105(1)	0.846(1)	7.0(4)*	C(214)	0.806(1)	0.252(1)	0.3564(8)	4.9(3)*
C(21d)	0.439(2)	−0.121(1)	0.776(1)	7.1(4)*	C(215)	0.772(1)	0.352(1)	0.3816(7)	4.0(3)*
C(21e)	0.434(1)	−0.033(1)	0.7075(9)	6.1(3)*	C(216)	0.770(1)	0.3506(9)	0.4660(9)	3.6(2)*
C(21f)	0.468(1)	0.078(1)	0.7082(7)	4.4(3)*	C(217)	0.881(1)	0.1294(9)	0.6808(6)	3.1(2)*
C(22)	0.613(1)	0.261(1)	0.8175(7)	3.6(3)*	C(218)	1.006(1)	0.127(1)	0.7109(7)	4.2(3)*
C(22a)	0.696(1)	0.237(1)	0.8868(7)	4.1(3)*	C(219)	1.053(1)	0.024(1)	0.7585(8)	5.4(3)*
C(22b)	0.780(2)	0.137(1)	0.8976(9)	6.6(4)*	C(220)	0.987(1)	−0.074(1)	0.7741(8)	5.4(3)*
C(22c)	0.863(2)	0.115(2)	0.960(1)	9.6(5)*	C(221)	0.872(1)	−0.075(1)	0.7434(8)	4.7(3)*
C(22d)	0.856(2)	0.191(2)	1.008(1)	8.8(5)*	C(222)	0.820(1)	0.0265(9)	0.6977(7)	3.8(2)*
$Co_2(CO)_4\{\eta^2,\eta^2,\eta^1,\eta^1\text{-}(Z)\text{-}Ph_2PC(Ph){=}(Ph)CC{=}C(PPh_2)C(O)OC(O)\}$									
Co(1)	0.8383(3)	0.1015(2)	0.4443(1)	1.87(5)*	C(11)	0.688(2)	0.045(1)	0.3463(9)	2.6(5)*
Co(2)	0.5943(3)	0.0876(2)	0.4208(1)	2.16(5)*	C(12)	0.601(2)	0.010(1)	0.3071(9)	2.8(5)*
P(1)	0.8127(6)	0.1199(3)	0.3501(2)	2.1(1)*	C(14)	0.606(2)	−0.088(1)	0.3770(8)	2.5(4)*
P(2)	0.6262(6)	0.0391(4)	0.5066(3)	2.3(1)*	C(15)	0.692(2)	−0.015(1)	0.396(1)	2.9(5)*
O(1)	1.113(2)	0.105(1)	0.4722(6)	4.1(4)*	C(16)	0.805(2)	−0.027(1)	0.4317(9)	2.2(5)*
O(2)	0.832(2)	0.275(1)	0.4822(7)	4.7(4)*	C(17)	0.786(2)	−0.004(1)	0.4937(9)	2.0(5)*
O(3)	0.323(2)	0.039(1)	0.4040(7)	5.7(4)*	C(111)	0.753(2)	0.220(1)	0.324(1)	3.4(6)*
O(4)	0.537(2)	0.268(1)	0.4235(7)	4.6(4)*	C(112)	0.820(2)	0.290(1)	0.3358(9)	3.1(5)*
O(12)	0.564(2)	0.033(1)	0.2603(7)	5.7(5)*	C(113)	0.789(3)	0.369(2)	0.313(1)	4.2(6)*
O(13)	0.545(1)	−0.0666(9)	0.3263(6)	3.5(4)*	C(114)	0.679(3)	0.374(2)	0.284(1)	5.2(7)*
O(14)	0.586(2)	−0.1543(9)	0.3993(7)	4.1(4)*	C(115)	0.601(3)	0.304(2)	0.268(1)	4.3(6)*
C(1)	1.004(2)	0.100(1)	0.4621(7)	1.7(4)*	C(116)	0.644(3)	0.222(2)	0.288(1)	4.4(6)*
C(2)	0.825(2)	0.204(1)	0.4698(8)	2.0(4)*	C(117)	0.943(2)	0.097(2)	0.2986(8)	2.8(5)*
C(3)	0.433(2)	0.059(1)	0.4083(9)	3.3(5)*	C(118)	0.922(2)	0.121(1)	0.2399(9)	3.4(5)*
C(4)	0.560(2)	0.199(1)	0.423(1)	3.1(5)*	C(119)	1.023(3)	0.110(2)	0.204(1)	5.4(7)*

Table 2 (Continued)

atom	x	y	z	B, Å^2	atom	x	y	z	B, Å^2
$Co_2(CO)_4\{\eta^2,\eta^2,\eta^1,\eta^1\text{-}(Z)\text{-}Ph_2PC(Ph){=}(Ph)CC{=}C(PPh_2)C(O)OC(O)\}$									
C(120)	1.142(3)	0.085(2)	0.219(1)	4.6(6)*	C(176)	0.923(2)	0.009(1)	0.5825(9)	1.9(4)*
C(121)	1.158(2)	0.063(1)	0.2751(9)	2.7(5)*	C(211)	0.639(2)	0.098(1)	0.5740(8)	2.3(4)*
C(122)	1.064(2)	0.068(1)	0.3139(9)	3.6(6)*	C(212)	0.641(2)	0.185(1)	0.5726(9)	3.2(5)*
C(161)	0.912(2)	−0.080(1)	0.4114(7)	1.6(4)*	C(213)	0.668(3)	0.227(2)	0.623(1)	4.6(6)*
C(162)	1.029(2)	−0.090(1)	0.4369(9)	3.7(5)*	C(214)	0.680(3)	0.184(2)	0.676(1)	5.6(7)*
C(163)	1.131(2)	−0.134(1)	0.4129(9)	3.6(6)*	C(215)	0.675(2)	0.101(2)	0.6751(9)	4.2(5)*
C(164)	1.116(3)	−0.172(2)	0.359(1)	5.1(7)*	C(216)	0.646(2)	0.057(1)	0.6231(9)	3.0(5)*
C(165)	1.003(3)	−0.159(2)	0.333(1)	5.6(7)*	C(217)	0.504(2)	−0.039(1)	0.5283(8)	1.8(4)*
C(166)	0.902(2)	−0.116(1)	0.3585(9)	3.0(5)*	C(218)	0.524(2)	−0.126(1)	0.5285(9)	3.3(5)*
C(171)	0.863(2)	−0.041(1)	0.5413(8)	1.8(4)*	C(219)	0.423(3)	−0.180(1)	0.544(1)	3.8(6)*
C(172)	0.857(2)	−0.128(1)	0.5480(9)	3.4(5)*	C(220)	0.308(2)	−0.151(1)	0.558(1)	3.0(5)*
C(173)	0.921(3)	−0.165(1)	0.595(1)	4.0(6)*	C(221)	0.286(3)	−0.067(2)	0.561(1)	5.3(7)*
C(174)	0.979(3)	−0.114(2)	0.634(1)	4.8(7)*	C(222)	0.386(3)	−0.010(1)	0.542(1)	4.0(6)*
C(175)	0.990(3)	−0.031(2)	0.629(1)	4.5(7)*					

[a] Asterisks indicate that atoms were refined isotropically. B values for anisotropically refined atoms are given in the form of the isotropic equivalent parameter defined as $(4/3)[a^2B(1,1) + b^2B(2,2) + c^2B(3,3) + ab(\cos\gamma)B(1,2) + ac(\cos\beta)B(1,3) + bc(\cos\alpha)B(2,3)]$.

by the work of Fenske[29] and Tyler[24,30] in addition to our MO calculations (vide infra).

4 exhibits similar reductive CV behavior with respect to the isomers of **2**, showing two redox waves at $E_{1/2} = -0.82$ and -1.53 V. The assignments for these waves are the same as those for **2** (i.e., bma-based reductions). Unlike the quasi-reversible 0/+1 wave found in each isomer of **2** and **3**, an irreversible oxidation ($I_p{}^a = 1.06$ V) is recorded for **4**.

The CV of the parent alkyne complex **1** has also been recorded under conditions identical to those used for **2**–**4** and is included for comparative purposes only (Table 4), as the electrochemical behavior of **1** has been fully explored.[27a] In CH_2Cl_2 solvent, both the oxidation and reduction waves are irreversible at a scan rate of 0.1 V s^{-1}. Since substitution of two CO ligands in **1** by P ligands is anticipated to decrease the reduction potential of **1** by ~0.2 V per P ligand,[31] the absence of a reduction wave for **3** is not surprising. However, the observation of multiple reduction waves for both isomers of **2** and **4** surely attests to the ability of the bma ligand to control the electron transfer process by stabilizing the added electron in a low-energy π^* orbital associated with the anhydride ring. The CV responses of the bma ligand have been included in Table 4, and the presence of two reduction waves at potentials close to those reported for the binuclear complexes **2** and **4** supports the LUMO as being a primarily bma-based orbital.

2 (chelating) was also examined by constant-potential coulometry in order to verify the electron stoichiometry associated with the 0/−1 redox couple and to explore the effect of electron accession on the IR stretching bands of the CO and bma ligands. **2** was reduced electrochemically at −0.65 V in CH_2Cl_2 solvent containing 0.1 M TBAP at −20 °C. The total charge passed upon completion of the reduction was $Q = 0.97$ C/mol of **2** in agreement with the one-electron nature of this redox couple. IR analysis of the catholyte at −20 °C shows the presence of four new ν(CO) bands at 2031 (vs), 1972 (vs), 1722 (s), and 1638 (s) cm^{-1}. The former two bands belong to the same terminal carbonyl groups already described for neutral **2** (chelating) but shifted by 16 and 21 cm^{-1} to lower frequency. This slight shift observed in the terminal CO bands indicates that only a small amount of the added electron density is associated with these CO groups.[32] A much larger shift is found in the latter two bma ν(CO) bands, which reveals that extensive odd-electron density is delocalized in the anhydride ring of the bma ligand.[24,29,30] In view of the current thinking on 18+δ complexes put forth by Brown[33] and Tyler,[24,30] the radical anion derived from each isomer of **2** can be considered as a 36+δ complex, as opposed to a formal 37-electron complex.[34]

V. Extended Hückel Calculations. The nature of the HOMO and LUMO in both isomers of **2** and **3** was determined by carrying out extended Hückel molecular orbital calculations. For simplicity, the phenyl groups associated with the acetylene and diphosphine ligands were replaced by hydrogen groups. Figure 3 shows the three-dimensional CACAO drawing of these molecular orbitals along with their respective energies.

In each binuclear complex examined, the HOMO, which is found at ~−11.9 eV, can best be described as a metal-based orbital that is composed of an in-phase overlap of hybridized d_{yz} orbitals. The nature of this hybridization has been fully analyzed by Hoffmann and co-workers in an earlier paper on the parent complex $Co_2(CO)_6(\mu\text{-}HC{\equiv}CH)$.[22,28,35,36] More importantly, our calculations clearly reveal that the LUMO in both isomers of **2** resides primarily on the bma ligand, in full agreement with our electrochemical data and the 36+δ formalism ascribed to the one-electron reduction product

---

(27) (a) Arewgoda, M.; Rieger, P. H.; Robinson, B. H.; Simpson, J.; Visco, S. J. *J. Am. Chem. Soc.* **1982**, *104*, 5633. (b) See also: Dickson, R. S.; Peake, B. M.; Rieger, P. H.; Robinson, B. H.; Simpson, J. *J. Organomet. Chem.* **1979**, *172*, C63.

(28) Hoffman, D. M.; Hoffmann, R.; Fisel, C. R. *J. Am. Chem. Soc.* **1982**, *104*, 3858.

(29) Fenske, D. *Chem. Ber.* **1979**, *112*, 363.

(30) (a) Tyler, D. R. *Acc. Chem. Res.* **1991**, *24*, 325. (b) Tyler, D. R.; Mao, F. *Coord. Chem. Rev.* **1990**, *97*, 119. (c) Mao, F.; Sur, S. K.; Tyler, D. R. *Organometallics* **1991**, *10*, 419. (d) Mao, F.; Tyler, D. R.; Rieger, A. L.; Rieger, P. H. *J. Chem. Soc., Faraday Trans.* **1991**, *87*, 3113.

(31) (a) Richmond, M. G.; Kochi, J. K. *Inorg. Chem.* **1986**, *25*, 656. (b) Hinkelmann, K.; Heinze, J.; Schacht, H.-T.; Field, J. S.; Vahrenkamp, H. *J. Am. Chem. Soc.* **1989**, *111*, 5078. (c) Ohst, H. H.; Kochi, J. K. *J. Am. Chem. Soc.* **1986**, *108*, 2897.

(32) (a) Don, M.-J.; Richmond, M. G. *Inorg. Chem.* **1991**, *30*, 1703. (b) Dumond, D. S.; Richmond, M. G. *J. Am. Chem. Soc.* **1988**, *110*, 7548. (c) Don, M.-J.; Richmond, M. G. *Inorg. Chim. Acta* **1990**, *173*, 61. (d) Peake, B. M.; Robinson, B. H.; Simpson, J.; Watson, D. J. *Inorg. Chem.* **1977**, *16*, 405. (e) Peake, B. M.; Rieger, P. H.; Robinson, B. H.; Simpson, J. *Inorg. Chem.* **1979**, *18*, 1000.

(33) Brown, T. L. In *Organometallic Radical Processes*; Trogler, W. C., Ed.; Elsevier: New York, 1990; Chapter 3 and reference therein.

(34) Extrapolation of the EAN formalism for mononuclear complexes to dinuclear complexes requires that both isomers of $2^{-\bullet}$ be designated as 36+δ complexes.

(35) For related studies on M_2L_6 binuclear systems, see: (a) Albright, T. A.; Hoffmann, R. *J. Am. Chem. Soc.* **1978**, *100*, 7736. (b) DeKock, R. L.; Deshmukukh, P.; Dutta, T. K.; Fehlner, T. P.; Housecroft, C. E.; Hwang, J. L.-S. *Organometallics* **1983**, *2*, 1108. (c) Anderson, A. B. *Inorg. Chem.* **1976**, *15*, 2598.

Table 3. Selected Bond Distances (Å) and Angles (deg) in the Binuclear Complexes 2-4[a]

$Co_2(CO)_4(\mu\text{-}PhC{\equiv}CPh)(bma){\cdot}CH_2Cl_2$ (Bridging Isomer)			
Bond Distances			
Co(1)—Co(2)	2.469(4)	Co(1)—P(1)	2.223(6)
Co(1)—C(1)	1.77(3)	Co(1)—C(2)	1.71(2)
Co(1)—C(5)	1.91(2)	Co(1)—C(6)	2.01(2)
Co(2)—P(2)	2.214(5)	Co(2)—C(3)	1.75(3)
Co(2)—C(4)	1.65(2)	Co(2)—C(5)	1.91(2)
Co(2)—C(6)	1.93(2)	P(1)—C(11)	1.81(2)
P(2)—C(15)	1.78(2)	O(1)—C(1)	1.15(3)
O(2)—C(2)	1.18(3)	O(3)—C(3)	1.15(3)
O(4)—C(4)	1.21(3)	O(12)—C(12)	1.19(3)
O(13)—C(12)	1.38(3)	O(13)—C(14)	1.32(3)
O(14)—C(14)	1.21(3)	C(5)—C(6)	1.29(3)
C(11)—C(12)	1.48(3)	C(11)—C(15)	1.42(3)
C(14)—C(15)	1.48(3)		
Bond Angles			
Co(2)—Co(1)—P(1)	108.3(2)	P(1)—Co(1)—C(1)	109.4(6)
P(1)—Co(1)—C(2)	97.0(8)	P(1)—Co(1)—C(5)	138.2(7)
P(1)—Co(1)—C(6)	100.0(6)	C(1)—Co(1)—C(2)	97(1)
Co(1)—Co(2)—P(2)	96.8(2)	P(2)—Co(2)—C(3)	106.6(6)
P(2)—Co(2)—C(4)	103.4(8)	P(2)—Co(2)—C(5)	142.9(5)
P(2)—Co(2)—C(6)	110.8(5)	C(3)—Co(2)—C(4)	99(1)
Co(1)—P(1)—C(11)	115.6(6)	Co(2)—P(2)—C(15)	113.3(6)
Co(1)—C(1)—O(1)	177(2)	Co(1)—C(2)—O(2)	179(3)
Co(2)—C(3)—O(3)	169(2)	Co(2)—C(4)—O(4)	175(2)
$Co_2(CO)_4(\mu\text{-}PhC{\equiv}CPh)\{(Z)\text{-}Ph_2PCH{=}CHPPh_2\}$			
Bond Distances			
Co(1)—Co(2)	2.485(2)	Co(1)—P(1)	2.237(3)
Co(1)—P(2)	2.188(3)	Co(1)—C(1)	1.78(1)
Co(1)—C(21)	1.930(9)	Co(1)—C(22)	1.92(1)
Co(2)—C(2)	1.77(1)	Co(2)—C(3)	1.79(1)
Co(2)—C(4)	1.71(1)	Co(2)—C(21)	1.99(1)
Co(2)—C(22)	1.98(1)	O(1)—C(1)	1.15(2)
O(2)—C(2)	1.16(2)	O(3)—C(3)	1.13(2)
O(4)—C(4)	1.17(1)	C(11)—C(12)	1.31(2)
Bond Angles			
P(1)—Co(1)—P(2)	87.7(1)	P(1)—Co(1)—C(1)	106.6(4)
P(2)—Co(1)—C(1)	96.8(4)	C(2)—Co(2)—C(3)	104.2(6)
C(2)—Co(2)—C(4)	103.8(7)	C(3)—Co(2)—C(4)	98.5(7)
Co(1)—C(1)—O(1)	171.8(9)	Co(2)—C(2)—O(2)	179(1)
Co(2)—C(3)—O(3)	175(1)	Co(2)—C(4)—O(4)	176(1)
$Co_2(CO)_4\{\eta^2,\eta^2,\eta^1,\eta^1\text{-}(Z)\text{-}Ph_2PC(Ph){=}(Ph)C\overline{C{=}C(PPh_2)C(O)OC}(O)\}$			
Bond Distances			
Co(1)—Co(2)	2.594(4)	Co(1)—P(1)	2.244(6)
Co(1)—C(1)	1.77(2)	Co(1)—C(2)	1.73(2)
Co(1)—C(16)	2.09(2)	Co(1)—C(17)	2.11(2)
Co(2)—P(2)	2.179(6)	Co(2)—C(3)	1.76(2)
Co(2)—C(4)	1.81(2)	Co(2)—C(11)	2.11(2)
Co(2)—C(15)	2.00(2)	P(1)—C(11)	1.76(2)
P(2)—C(17)	1.81(2)	O(1)—C(1)	1.16(2)
O(2)—C(2)	1.17(3)	O(3)—C(3)	1.19(3)
O(4)—C(4)	1.12(3)	O(12)—C(12)	1.22(3)
O(13)—C(12)	1.42(3)	O(13)—C(14)	1.39(2)
O(14)—C(14)	1.19(3)	C(11)—C(12)	1.40(3)
C(11)—C(15)	1.50(3)	C(14)—C(15)	1.53(3)
C(15)—C(16)	1.45(3)	C(16)—C(17)	1.51(3)
Bond Angles			
Co(2)—Co(1)—P(1)	71.8(2)	Co(2)—Co(1)—C(1)	174.3(7)
Co(2)—Co(1)—C(2)	94.3(7)	C(1)—Co(1)—C(2)	90(1)
C(1)—Co(1)—C(16)	100.5(9)	C(1)—Co(1)—C(17)	96.5(9)
C(2)—Co(1)—C(16)	161.5(9)	C(2)—Co(1)—C(17)	122.2(9)
P(2)—Co(2)—C(15)	84.5(7)	C(3)—Co(2)—C(4)	94(1)
C(4)—Co(2)—C(11)	115.5(9)	C(4)—Co(2)—C(15)	155(1)
Co(1)—P(1)—C(11)	92.7(7)	Co(1)—C(1)—O(1)	175(2)
Co(1)—C(2)—O(2)	170(2)	Co(2)—C(3)—O(3)	175(2)
Co(2)—C(4)—O(4)	178(2)	C(15)—C(16)—C(17)	115(2)

[a] Numbers in parentheses are estimated standard deviations in the least significant digits.

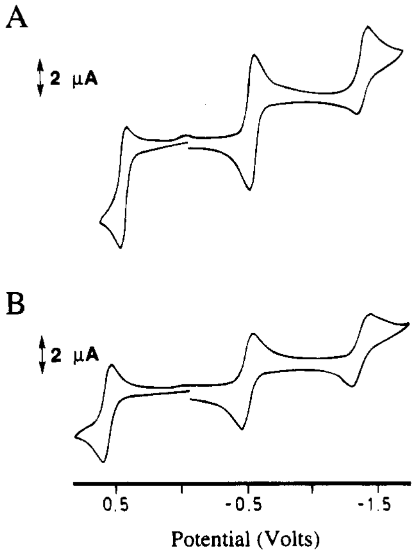

Figure 2. Anodic scan cyclic voltammogram of (A) **2** (chelating) (ca. 3.2 × 10^{-3} M) and (B) **2** (bridging) (ca. 1.9 × 10^{-3} M) in CH_2Cl_2 containing 0.1 M TBAP at 100 mV/s.

derived from **2**. The nodal pattern of the bma ligand in each LUMO of **2** can be envisioned as arising from ψ_4 of an isolated six π-electron system (e.g., maleic anhydride or hexatriene).[37] The LUMO energy for each of these binuclear complexes is calculated at ~−10.4 eV and is substantially below the LUMO of **3**, which does not possess a redox-active diphosphine ligand.

The LUMO in **3** is represented by an out-of-phase overlap of hybridized d_{yz} orbitals, with a contribution from the acetylene π bond. This LUMO is the same as that calculated by Hoffmann and co-workers for $Co_2(CO)_6(\mu\text{-}HC{\equiv}CH)$[28] and is best described as an antibonding Co—Co orbital, whose energy is ~−9.9 eV. The effect of the unsaturated ethano bridge on the HOMO and LUMO in **3** was also probed by conducting calculations on the model compound $Co_2(CO)_4(PH_3)_2(\mu\text{-}HC{\equiv}CH)$ (1,1-substitution). The calculated HOMO and LUMO energy levels and the orbital compositions exhibited no major perturbations from those data obtained from **3**.

Discussion

The binuclear cobalt complex $Co_2(CO)_6(\mu\text{-}PhC{\equiv}CPh)$ reacts with the diphosphine ligand bma in the presence of Me_3NO at room temperature to yield the dinuclear complex $Co_2(CO)_4(\mu\text{-}PhC{\equiv}CPh)$(bma), which contains a

---

(36) The subjacent HOMO in compounds **2** (both isomers) and **3** consists of a Co—Co antibonding orbital derived from the out-of-phase overlap of hybridized d_{xz} orbitals, with a minor contribution from the acetylene π^* bond. The switching of our HOMO and the subjacent HOMO from that in ref 28 is immaterial, insomuch as the overall bonding in this genre of binuclear compounds is not adversely perturbed. The energy level for each subjacent HOMO in **2** and **3** is calculated at ~−12.1 eV.

(37) In agreement with our premise concerning the LUMO of **2**, the calculated energy (−10.4 eV) and the nodal properties of the LUMO of maleic anhydride closely match those reported here for bma-substituted **2**. See also: Hayakawa, K.; Mibu, N.; Ōsawa, E.; Kanematsu, K. *J. Am. Chem. Soc.* **1982**, *104*, 7136.

(38) For reports on P—C bond cleavage reactions, see: (a) Garrou, P. E. *Chem Rev.* **1985**, *85*, 171. (b) Carty, A. J. *Pure Appl. Chem.* **1982**, *54*, 113. (c) Etienne, M.; Mathieu, R.; Lugan, N. *Organometallics* **1993**, *12*, 140. (d) Corrigan, J. F.; Doherty, S.; Taylor, N. J.; Carty, A. J. *Organometallics* **1993**, *12*, 1365. (e) Harley, A. D.; Guskey, G. J.; Geoffroy, G. L. *Organometallics* **1983**, *2*, 53. (f) Dubois, R. A.; Garrou, P. E. *Organometallics* **1986**, *5*, 466. (g) Bruce, M. I. *J. Organomet. Chem.* **1990**, *394*, 365. (h) Bruce, M. I.; Williams, M. L.; Patrick, J. M.; Skelton, B. W.; White, A. H. *J. Chem. Soc., Dalton Trans.* **1986**, 2557. (i) Lugan, N.; Bonnet, J.-J.; Ibers, J. A. *J. Am. Chem. Soc.* **1985**, *107*, 4484. (j) McGhee, W. D.; Foo, T.; Hollander, F. J.; Bergman, R. G. *J. Am. Chem. Soc.* **1988**, *110*, 8543.

(39) Conole, G.; Hill, K. A.; McPartlin, M.; Mays, M. J.; Morris, M. J. *J. Chem. Soc., Chem. Commun.* **1989**, 688.

Table 4. Cyclic Voltammetry Data[a] for 2-4, $Co_2(CO)_6(\mu\text{-}PhC{\equiv}CPh)$, and bma

	redox couple[b]								
	0/+1			0/−1			−1/−2		
compd	E_p^a	E_p^c	$E_{1/2}$	E_p^c	E_p^a	$E_{1/2}$	E_p^c	E_p^a	$E_{1/2}$
2 (chelating)	0.48	0.39	0.44	−0.61	−0.53	−0.57	−1.50	−1.39	−1.45
2 (bridging)	0.61	0.53	0.57	−0.56	−0.47	−0.52	−1.47	−1.33	−1.40
3	0.26	0.18	0.22						
4	1.06			−0.87	−0.77	−0.82	−1.62	−1.44	−1.53
$Co_2(CO)_6(\mu\text{-}PhC{\equiv}CPh)$[c]	0.98			−1.35					
bma (free ligand)[d]				−0.67	−0.58	−0.63	−1.44	−1.32	−1.38

[a] In ~10^{-3} M CH_2Cl_2 solutions containing 0.1 M TBAP at room temperature and a scan rate of 0.1 V s^{-1}. Potentials are in volts relative to a silver wire quasi-reference electrode, calibrated against ferrocene. [b] E_p^a and E_p^c refer to the anodic and cathodic peak potentials of the CV waves. The half-wave potential $E_{1/2}$, which represents the chemically reversible redox couple, is defined as $(E_p^a + E_p^c)/2$. [c] See ref 27. [d] See ref 24a.

chelating bma ligand. The identity of this product has been established by IR and NMR (^{13}C and ^{31}P) spectroscopies. Equilibration of the chelating isomer to the bridging isomer of **2** occurs upon thermolysis. We have recently shown that reversible chelate-to-bridge bma ligand exchange is possible in $PhCCo_3(CO)_7(bma)$.[12] As in the case of $PhCCo_3(CO)_7(bma)$, we believe that the uncoordinated bma C=C bond is crucial for the successful isomerization of the bma ligand in **2**.

The absence of facile diphosphine isomerization in **3** is of interest, as we believe that this highlights one of the unique reactivity differences between the bma ligand and normal diphosphine ligands devoid of an electron-withdrawing substituent(s). Heating or photolyzing solutions of **3** leads only to the decomposition of **3**, presumably due to the retarded ability of the (*Z*)-$Ph_2PCH{=}CHPPh_2$ diphosphine ligand to enter into the P—C bond cleavage reaction available to the bma ligand. Analogous reactivity has been reported by us for $PhCCo_3(CO)_7$(P-P) (where P-P = bma, (*Z*)-$Ph_2PCH{=}CHPPh_2$).[12]

The low yield associated with the production of **4** stands in contrast to the bma/cluster activation reported for $PhCCo_3(CO)_7(bma)$.[12] Although the exact reason(s) for the low yield of **4** is (are) unknown, it is likely that the oxidative addition of the P—C(olefin) bond and/or phosphido attack on the alkyne carbon are less favorable in the dinuclear case compared to the trinuclear cluster.[12] We are currently examining the reactivity of the bma ligand in other systems in order to gain a greater understanding of the factors that influence the P—C bond cleavage in this particular ligand.[38,39]

The nature of the ancillary P ligand in **4** is related to the complexes obtained from the reaction between $Co_2(CO)_6(\mu_2\text{-}PPh_2)_2$ and alkynes.[40,41] Double insertion of the alkyne into the Co-phosphido bond leads to the metallocyclic complexes $Co_2\{\mu\text{-}Ph_2PCRCR'C(O)CR''CR'''PPh_2\}(CO)_4$. The nine-membered ring, which tethers both of the $Co(CO)_2$ groups, is identical to our eight-electron ligand $\eta^2,\eta^2,\eta^1,\eta^1$-(*Z*)-$Ph_2PC(Ph){=}(Ph)CC{=}C(PPh_2)C(O)OC(O)$ in **4**, except for the presence of the inserted carbonyl group.

Experimental Section

General Procedures. $Co_2(CO)_8$ was purchased from Strem Chemical Co., while diphenylacetylene and 2,3-dichloromaleic anhydride were obtained from Aldrich Chemical Co. $Co_2(CO)_6(\mu\text{-}PhC{\equiv}CPh)$[42] and Ph_2PTMS[43] were prepared according to the published literature procedures. The bma ligand was synthesized by using the procedure of Tyler.[24b] All reactions were conducted under argon using Schlenk techniques.[44] THF and toluene were distilled from sodium/benzophenone ketyl, while CH_2Cl_2 and dichloroethane were distilled from CaH_2. All distilled solvents were stored under argon in Schlenk storage vessels equipped with Teflon stopcocks. The ^{13}CO (>99%) used to prepare the isotopically enriched $Co_2(CO)_6(\mu\text{-}PhC{\equiv}CPh)$ was obtained from Isotec.

Infrared spectra were recorded on a Nicolet 20SXB FT-IR spectrometer. Routine room temperature spectra were recorded in 0.1-mm NaCl cells. Low-temperature IR spectra were recorded with a Specac Model P/N 21.000 variable-temperature cell equipped with inner and outer CaF_2 windows. Dry ice/acetone was used a coolant, and the reported cell temperature was measured by using a copper—constantan thermocouple. The ^{13}C and ^{31}P NMR spectra were recorded on a Varian 300-VXR spectrometer at 75 and 121 MHz, respectively. The reported ^{31}P chemicals shifts are referenced relative to external H_3PO_4 (85%) taken to have $\delta = 0$. Positive chemical shifts signify resonances that are low field to the external standard.

Synthesis of $Co_2(CO)_4(\mu\text{-}PhC{\equiv}CPh)(bma)$ (Chelating Isomer). To a mixture of 0.50 g of $Co_2(CO)_6(\mu\text{-}PhC{\equiv}CPh)$ (1.08 mmol) and 0.50 g of bma (1.07 mmol) in 50 mL of THF was added 0.16 g of Me_3NO (2.13 mmol). An immediate color change from brown to black-green was observed, and the reaction was shown to be complete after 1 h by IR spectroscopy and TLC analysis. The reaction solution was dried under vacuum and then purified by chromatography over silica gel using CH_2Cl_2/petroleum ether (3:1) at −78 °C. The analytical sample was recrystallized from a 1:1 mixture of CH_2Cl_2 and pentane. Attempts to grow single crystals of **2** (chelating) suitable for X-ray diffraction analysis were unsuccessful. Yield: 0.65 g (69%). IR (CH_2Cl_2): ν(CO) 2047 (vs), 1993 (vs), 1952 (sh), 1842 (w, asymm bma C=O), 1775 (s, symm bma C=O) cm^{-1}. $^{31}P\{^1H\}$ NMR ($CDCl_3$, −56 °C): δ 60.3. $^{13}C\{^1H\}$ NMR (THF, −91 °C): δ 207.5 (1C, bma-substituted cobalt), 201.1 (3C, $Co(CO)_3$). Anal. Calcd (found) for $C_{46}H_{30}Co_2O_7P_2\cdot 0.5CH_2Cl_2$: C, 60.84 (60.73); H 3.49 (3.40).

Synthesis of $Co_2(CO)_4(\mu\text{-}PhC{\equiv}CPh)(bma)$ (Bridging Isomer). To a Schlenk tube containing 0.20 g of the chelating isomer of $Co_2(CO)_4(\mu\text{-}PhC{\equiv}CPh)(bma)$ (0.23 mmol) was added 40 mL of 1,2-dichloroethane, after which the solution was heated overnight at 45 °C. The IR spectrum of the cooled solution revealed the presence of a 1:1 mixture of chelating and bridging **2**. Due to inefficient compound separation on

---

(40) (a) Caffyn, A. J. M.; Mays, M. J.; Solan, G. A.; Braga, D.; Sabatino, P.; Tiripicchio, A., Tiripicchio-Camellini, M. *Organometallics* **1993**, *12*, 1876. (b) Also see: ref 39.

(41) (a) Caffyn, A. J. M.; Mays, M. J.; Solan, G. A.; Conole, G.; Tiripicchio, A. *J. Chem. Soc., Dalton Trans.* **1993**, 2345. (b) For a report on alkyne insertion into a μ-phosphido bond of a RuCo binuclear complex, see: Regragui, R.; Dixneuf, P. H.; Taylor, N. J.; Carty, A. J. *Organometallics* **1990**, *9*, 2234.

(42) Bor, G.; Kettle, S. F. A.; Stanghellini, P. L. *Inorg. Chim. Acta* **1976**, *18*, L18.

(43) Kuchen, W.; Buchwald, H. *Chem. Ber.* **1959**, *92*, 227.

(44) Shriver, D. F. *The Manipulation of Air-Sensitive Compounds*; McGraw-Hill: New York, 1969.

(45) (a) Hoffmann, R. *J. Chem. Phys.* **1963**, *39*, 1397. (b) Hoffmann, R.; Libscomb, W. N. *J. Chem. Phys.* **1962**, *36*, 3179.

(46) Mealli, C.; Proserpio, D. M. *J. Chem. Educ.* **1990**, *67*, 399.

(47) Ammeter, J. H.; Bürgi, H.-B.; Thibeault, J. C.; Hoffmann, R. *J. Am. Chem. Soc.* **1978**, *100*, 3686.

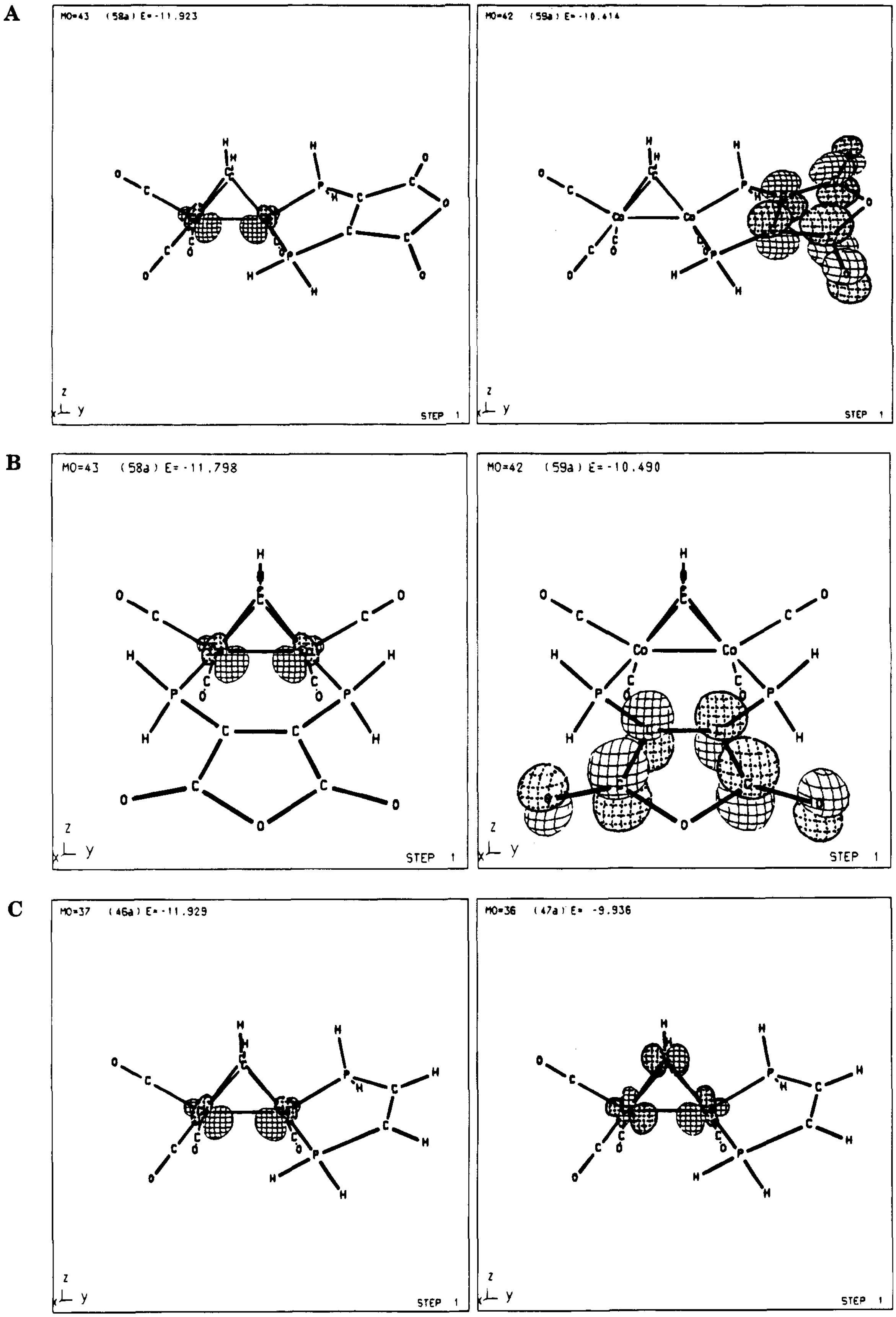

Figure 3. CACAO drawings of the HOMO (left) and the LUMO (right) for (A) $Co_2(CO)_4(\mu\text{-}HC{\equiv}CH)(H_4\text{-bma})$ (chelating), (B) $Co_2(CO)_4(\mu\text{-}HC{\equiv}CH)(H_4\text{-bma})$ (bridging), and (C) $Co_2(CO)_4(\mu\text{-}HC{\equiv}CH)\{(Z)\text{-}H_2PCH{=}CHPH_2\}$ (chelating).

silica gel, column chromatography could not be employed in the purification of this isomeric mixture. The solvent was instead removed under vacuum, followed by repeated crystallizations using CH_2Cl_2/petroleum ether. By this method, pure **2** (bridging) was ultimately isolated from the mother liquor in pure form. The analytical sample was recrystallized from CH_2Cl_2/pentane (1:1) to give 0.02 g (yield 10%) of $Co_2(CO)_4(\mu\text{-}PhC{\equiv}CPh)$(bma) (bridging). IR ($CH_2Cl_2$): ν(CO) 2031 (s), 2009 (vs), 1982 (sh), 1818 (w, asymm bma C=O), 1765 (s, symm bma C=O) cm^{-1}. $^{31}P\{^1H\}$ NMR (THF, −91 °C): δ 30.5. ^{13}C-

{^{1}H} NMR (THF, −91 °C): δ 203.2 (4C, two $Co(CO)_2$ groups). Anal. Calcd (found) for $C_{46}H_{30}Co_2O_7P_2{\cdot}CH_2Cl_2$: C, 58.48 (58.83); H 3.49 (3.36).

Synthesis of $Co_2(CO)_4(\mu\text{-}PhC{\equiv}CPh)$\{(*Z*)-$Ph_2PCH{=}CHPPh_2$\}. To 0.20 g of $Co_2(CO)_6(\mu\text{-}PhC{\equiv}CPh)$ (0.43 mmol), 0.17 g of (*Z*)-$Ph_2PCH{=}CHPPh_2$ (0.43 mmol), and 64.5 mg of Me_3NO (0.86 mmol) in a Schlenk tube was added 50 mL of CH_2Cl_2. Stirring was continued for 3 h, after which time IR analysis indicated the presence of product (>90%). The desired product was isolated by chromatography over silica gel using CH_2Cl_2/petroleum ether (1:1) and was then recrystallized from CH_2Cl_2/pentane (1:1) to give green-black **3**. Yield: 0.25 g (73%). IR (CH_2Cl_2): ν(CO) 2039 (vs), 1983 (vs) cm^{-1}. ^{31}P{^{1}H} NMR (THF, −91 °C): δ 71.8. ^{13}C{^{1}H} NMR (THF, −91 °C): δ 208.8 (1C, P_2-substituted cobalt), 202.8 (3C, $Co(CO)_3$). Anal. Calcd (found) for $C_{44}H_{32}Co_2O_4P_2$: C, 65.68 (65.77); H 4.01 (4.01).

Synthesis of $Co_2(CO)_4\{\eta^2,\eta^2,\eta^1,\eta^1$-(*Z*)-$Ph_2PC(Ph){=}(Ph)CC{=}C(PPh_2)C(O)OC(O)\}$. To 0.25 g of $Co_2(CO)_6(\mu\text{-}PhC{\equiv}CPh)$ (0.54 mmol) and 0.25 g of bma (0.54 mmol) was added 1,2-dichloroethane by syringe, after which the solution was refluxed for 5 h. After the solution was allowed to cool to room temperature, TLC analysis revealed the presence of only one slow moving spot. This material was subsequently isolated by column chromatography over silica gel using CH_2Cl_2 as the eluant. The isolated red-brown complex **4** was recrystallized from CH_2Cl_2/pentane (1:1) to give pure **4**. Yield: 0.05 g (10%). IR (CH_2Cl_2): ν(CO) 2050 (s), 2025 (vs), 2008 (s), 1981 (m), 1809 (w, asymm bma C=O), 1745 (m, symm bma C=O) cm^{-1}. ^{31}P{^{1}H} NMR (THF, −91 °C): δ 46.7 (1P), 27.8 (1P, d, J = 17.0 Hz). ^{13}C{^{1}H} NMR (THF, −91 °C): δ 202.1 (1C,), 201.1 (1C, d, J = 15.3 Hz), 196.9 (1C), 193.7 (1C). Anal. Calcd (found) for $C_{46}H_{30}Co_2O_7P_2$: C, 62.82 (63.18); H 3.94 (3.46).

X-ray Diffraction Structure of $Co_2(CO)_4(\mu\text{-}PhC{\equiv}CPh)(bma){\cdot}CH_2Cl_2$ (Bridging Isomer). Crystals suitable for X-ray diffraction analysis were grown from a CH_2Cl_2 solution containing **2** (bridging) that had been layered with heptane. The selected crystal, of dimensions 0.08 × 0.08 × 0.42 mm^3, was sealed inside a Lindemann capillary and then mounted on an Enraf-Nonius CAD-4 diffractometer. Cell constants were obtained from a least-squares refinement of 25 reflections with $2\theta > 24°$. Intensity data in the range $2.0 \le 2\theta \le 44°$ were collected at 298 K using the ω-scan technique in the variable-scan speed mode and were corrected for Lorentz, polarization, and absorption (DIFABS). Three reflections (400, 060, 004) were measured after every 3600 s of exposure time in order to monitor crystal decay (<2%). The structure was solved by SIR, which revealed the positions of the Co and P atoms. All remaining non-hydrogen atoms were located with difference Fourier maps and full-matrix least-squares refinement. With the exception of the cobalt and phosphorus atoms, all atoms were refined isotropically. Refinement converged at R = 0.0697 and R_w = 0.0850 for 1711 unique reflections with $I > 3\sigma(I)$.

X-ray Diffraction Structure of $Co_2(CO)_4(\mu\text{-}PhC{\equiv}CPh)$\{(*Z*)-$Ph_2PCH{=}CHPPh_2$\}. A black crystal of dimensions 0.08 × 0.11 × 0.22 mm^3 was prepared in a manner similar to that described for **2** (bridging). Cell constants were obtained from a least-squares refinement of 25 reflections with $2\theta > 25°$. Intensity data in the range $2.0 \le 2\theta \le 44°$ were collected at 298 K using the $\theta/2\theta$-scan technique in the variable-scan speed mode and were corrected for Lorentz, polarization, and absorption (DIFABS). Three reflections (500, 060, 006) were measured after every 3600 s of exposure time in order to monitor crystal decay (<2%). The structure was solved by SIR, which revealed the positions of the Co and P atoms. All remaining non-hydrogen atoms were located with difference Fourier maps and full-matrix least-squares refinement. With the exception of the phenyl carbons, all non-hydrogen atoms were refined anisotropically. Refinement converged at R = 0.0587 and R_w = 0.0650 for 2425 unique reflections with $I > 3\sigma(I)$.

X-ray Diffraction Structure of $Co_2(CO)_4\{\eta^2,\eta^2,\eta^1,\eta^1$-(*Z*)-$Ph_2PC(Ph){=}(Ph)CC{=}C(PPh_2)C(O)OC(O)\}$. A black crystal of dimensions 0.04 × 0.22 × 0.31 mm^3 was prepared in a manner similar to that described for **2** (bridging). Cell constants were obtained from a least-squares refinement of 25 reflections with $2\theta > 25°$. Intensity data in the range $2.0 \le 2\theta \le 44°$ were collected at 298 K using the ω-scan technique in the variable-scan speed mode and were corrected for Lorentz, polarization, and absorption (DIFABS). Three reflections (600, 060, 0012) were measured after every 3600 s of exposure time in order to monitor crystal decay (<2%). The structure was solved by SIR, which revealed the positions of the Co and P atoms. All remaining non-hydrogen atoms were located with difference Fourier maps and full-matrix least-squares refinement and refined isotropically. Refinement converged at R = 0.0529 and R_w = 0.0608 for 1141 unique reflections with $I > 3\sigma(I)$.

Electrochemical Measurements. Cyclic voltammetric measurements were conducted by using a PAR Model 273 potentiosstat/galvanostat, equipped with positive feedback circuitry to compensate for *IR* drop. The cell used in the CV studies was of airtight design and based on a three-electrode configuration. All CV experiments employed a platinum disk (area = 0.0079 cm^2) as the working and auxiliary electrode. All voltammograms utilized a silver wire quasi-reference electrode, and all potential data are referenced relative to the formal potential of the Cp_2Fe/Cp_2Fe^+ (internally added) redox couple recorded under identical conditions, taken to have $E_{1/2}$ = 0.306 V.[25a]

The bulk electrolysis experiment involving **2** (chelating) was carried out in the constant-potential mode at −0.65 V in an airtight bulk-electrolysis cell at −20 °C in CH_2Cl_2 solvent containing 0.1 M TBAP. After the electrolysis was completed, the catholyte was examined by IR spectroscopy, using a low-temperature IR cell. At no time during the electrolysis or IR analysis was the solution temperature allowed to exceed −20 °C.

Extended Hückel Molecular Orbital Calculations. All calculations were carried out by using the original program developed by Hoffmann, as modified by Mealli and Proserpio, with weighted H_{ij}'s. The HOMO and LUMO orbitals shown in the paper were done with the CACAO drawing program of Mealli and Proserpio.

Acknowledgment. We are especially grateful to Prof. Carlo Mealli for furnishing M.G.R. with a copy of his CACAO graphics program and Prof. Roald Hoffmann for helpful correspondence. Financial support from the Robert A. Welch Foundation (Grant B-1202-SGB and B-1039-MGR) and the UNT Faculty Research Program is acknowledged.

Supplementary Material Available: Textual presentations of the crystallographic experimental details and listings of crystallographic data, bond distances, bond angles, and hydrogen positional and thermal parameters for $Co_2(CO)_4(\mu\text{-}PhC{\equiv}CPh)(bma)$, $Co_2(CO)_4(\mu\text{-}PhC{\equiv}CPh)$\{(*Z*)-$Ph_2PCH{=}CHPPh_2$\}, and $Co_2(CO)_4\{\eta^2,\eta^2,\eta^1,\eta^1$-(*Z*)-$Ph_2PC(Ph){=}(Ph)CC{=}C(PPh_2)C(O)OC(O)\}$ (42 pages). Ordering information is given on any current masthead page.

OM940203U